

Roles of the *C. elegans* cyclophilin-like protein MOG-6 in MEP-1 binding and germline fates

Marco Belfiore*, Paolo Pugnale*, Zarifja Saudan and Alessandro Puoti†

Department of Biology, Unit of Zoology, University of Fribourg, 1700 Fribourg, Switzerland

*These authors contributed equally to this work

†Author for correspondence (e-mail: Alessandro.Puoti@unifr.ch)

Accepted 2 March 2004

Development 131, 2935-2945
Published by The Company of Biologists 2004
doi:10.1242/dev.01154

Summary

The switch from spermatogenesis to oogenesis in the *Caenorhabditis elegans* hermaphrodite requires *mog-6*, which post-transcriptionally represses the *fem-3* RNA. In this study, we show that *mog-6* codes for a divergent nuclear cyclophilin, in that a conserved domain is not required for its function in the sperm-oocyte switch. MOG-6 binds to the nuclear zinc finger protein MEP-1 through two separate domains that are essential for the role of MOG-6 in the sperm-oocyte switch. We propose that

MOG-6 has a function distinct from that of prevailing cyclophilins and that its binding to MEP-1 is essential for germline sex determination. Finally, we found that *gld-3 mog-6* mutants develop germline tumors, suggesting that *mog-6* might function in the decision between mitosis and meiosis.

Key words: Cyclophilin, *mog-6*, *fem-3*, *gld-3*, *mep-1*, Germline development

Introduction

The *Caenorhabditis elegans* hermaphrodite produces sperm during larval development and switches to oogenesis as an adult (Schedl, 1997). The *fem-3* mRNA is active during spermatogenesis but is post-transcriptionally repressed through its 3'UTR for the switch to oogenesis (Ahringer and Kimble, 1991; Barton et al., 1987). The *mog* genes are required in vivo for *fem-3* repression, since their inactivation results in continuous production of sperm in hermaphrodites, a phenotype that is similar to that of *fem-3 gain-of-function (gf)* mutants (Barton et al., 1987; Graham and Kimble, 1993; Graham et al., 1993). Furthermore, the *mog* genes have been shown to function via the *fem-3* 3'UTR in vivo (Gallegos et al., 1998). The characterization of the *mog* genes represents one way to understand the molecular basis of *fem-3* regulation. *mog-1*, *mog-4* and *mog-5* encode proteins of a subclass of nuclear DEAH-box RNA helicases (Puoti and Kimble, 1999; Puoti and Kimble, 2000). The cytoplasmic RNA-binding proteins FBF, NOS-3 and GLD-3 and the nuclear zinc finger protein MEP-1 represent additional regulators of *fem-3*. While FBF and NOS-3 form a complex with the *fem-3* 3'UTR (Kraemer et al., 1999; Zhang et al., 1997), GLD-3 prevents FBF from binding to *fem-3* (Eckmann et al., 2002), and MEP-1 physically interacts with MOG-1, MOG-4 and MOG-5 (Belfiore et al., 2002).

Here we report that *mog-6* (*cyp-4* – WormBase) codes for a divergent cyclophilin widely expressed in somatic and germline nuclei. All cyclophilins harbor a conserved central binding domain (CBD) necessary for Cyclosporin A (CsA) binding and protein folding (Fischer et al., 1989; Handschumacher et al., 1984). We found that MOG-6 binds to MEP-1, and provide evidence that the CBD in MOG-6 is

neither necessary for MEP-1 binding nor for its role in germline sex determination.

Besides the sperm/oocyte decision, germ cells in the hermaphrodite also undergo a decision between mitotic proliferation and meiosis. We show that in the absence of *gld-3*, loss of *mog-6* causes germ cells to proliferate mitotically instead of differentiating into sperm, indicating that *mog-6* functions in the decision between mitosis and meiosis.

Materials and methods

Cloning of *mog-6*

mog-6 was mapped between *unc-4* and *sqt-1* using *mog-6(q465)/unc-4(e120) sqt-1(sc13) II* worms. We found that among 104 non-Unc roller recombinants, 66 were + *sqt-1/unc-4sqt-1* and 38 were *mog-6 sqt-1/unc-4 sqt-1*. Additional mapping was done using deletions. The right end of deletion *mnDf57* was located between cosmids T19E10 and M106 and the left end of *mnDf87* was in cosmid F44F4. Thus, *mog-6* was located in a region that was covered by cosmids T19E10, K03C1, F44F4, M106 and F59E10. *mog-6(q465) unc-4(e120)/mnC1* hermaphrodites were injected with 6 ng/μl of each cosmid, 30 ng/μl of pRF4 roller DNA and 70 ng/μl of *Haemophilus influenzae* DNA. Cosmid M106 rescued *mog-6*, since Unc fertile Rollers were obtained among the F1 and F2 progenies. *mog-6* was also rescued by a 3.1 kb PCR-generated fragment corresponding to the 3' end of M106 (pAP6 in Fig. 1). All genomic *mog-6* constructs, including mutated *mog-6* derivatives, were flanked by 515 and 823 nucleotides of genomic sequence on the 5' and the 3' end, respectively. MOG-6 derivatives containing N-terminal deletions did nevertheless include the first 10 amino acids of MOG-6 and therefore the translational initiation codon.

Double mutant strains

Progeny of *mog-6(q465)/sqt-1(sc13) II; mep-1(q660)IV/Dnt1[qIs50] (IV;V)* that was non-rolling, non-dumpy and not glowing was scored

for germline defects. *mog-6;mep-1* homozygotes occasionally made a few oocytes that were never fertilized and produced slightly higher amounts of sperm (255±50, $n=22$ gonadal arms analyzed; wild-type, 160 sperm per arm). Non-rolling, non-dumpy progeny of *fog-1(q253ts) I;mog-6(q465)/sqt-1(sc13) II* grown at 25°C was scored for germ cells. To obtain the total number of germ cells, the number of sperm was divided by four and added to the number of immature germ cells. The *mog-6 gld-3* double mutant was obtained by selecting non-dumpy non-unc progeny of a cross between a *dpy-10(e128)mog-6(q465)/gld-3(q730)unc-4(e120)* male and a *dpy-10(e128)unc-4(e128)* hermaphrodite. The *mog-6 gld-3* chromosome was balanced with a dominant GFP marker, *mIn1[dpy-10(e128)mIs14 GFP]*. Germ cells were counted in (4,6-diamidino-2-phenylindole) DAPI-stained animals 24 hours past L4.

Northern blotting and RT-PCR

PolyA-enriched RNA and total RNA were isolated from synchronized animals as described (Puoti and Kimble, 1999). Total RNA was treated by DNase for 30 minutes at 37°C (Stratagene). For northern analyses, polyA-enriched RNA or total RNA was resolved on a denaturing gel, blotted and probed with the entire corresponding cDNA, unless stated otherwise. For *act-1*, a 250 nt gene-specific fragment was used. CeIF that is expressed at constant levels during development was used as a loading control (Roussell and Bennett, 1992). The *gld-3* probe corresponded to the 5' end of the cDNA (nt 1-766).

For RT-PCR experiments, single-stranded cDNA was synthesized at 37°C using 1.5 µg of total RNA, 100 ng of random primers and 400 units Superscript II reverse transcriptase (Gibco BRL). 1/20 of each sample was used for PCR. For positive controls, 14 ng of genomic DNA and 44 ng of oligo(dT)-primed single-stranded cDNA from wild-type worms were used (Fig. 5A, lanes 1, 2, 7, 8, 13, 14, 19 and 20). Primer sequences are available upon request.

GFP reporter experiment

A *HpaI* site was created 9 nt upstream of the *mog-6* stop codon in pAP6. A 1091-nt *SmaI-SspI* fragment of *gfp* was cloned into the *HpaI* site. pAP7 contained the stop codon of *gfp* and the 5' and 3' flanking regions of the *mog-6* gene (Fig. 3B). pAP7 was injected into *mog-6* heterozygotes at 5.6 ng/µl. Roller lines were scored by epifluorescence.

Preparation of antibodies and immunostaining

Anti-MOG-6 antibodies were raised in a rabbit using a GST-tagged MOG-6 polypeptide (AA₁₋₃₀₂). MOG-6 antibodies were purified by Western blotting on a HIS-tagged MOG-6 fusion protein. Anti-FBF, anti-GLD-3 and anti-NOS-3 antibodies were kindly provided by Judith Kimble (Eckmann et al., 2002; Kraemer et al., 1999; Zhang et al., 1997). For western blotting, approximately 15 mg of total worm protein extract were loaded per lane. Equal loading was verified by staining with Ponceau S. Purified anti-MOG-6 antibodies were used at a dilution of 1:30. HRP-coupled secondary antibodies HRP (Sigma) were used at 1:15 000 in Blotto/Tween. For immunocytochemistry, purified anti-MOG-6 antibodies were diluted 1:10. The secondary antibody was either anti-rabbit IgG Cyanine conjugate or anti-rabbit IgG FITC conjugate (Jackson ImmunoResearch) diluted 1:1000. Immunostainings were performed either on entire animals (Bettinger et al., 1996) or on dissected gonads (Francis et al., 1995; Jones et al., 1996). Stained worms were mounted with Vectashield (Vector) containing 2 µg/ml DAPI and observed under fluorescence. The anti-phospho-histone H3 antibody (Upstate) was used at 1/100.

Protein-protein interaction assays

For yeast two-hybrid interaction assays, the coding sequences for the MOG-6 and derivatives thereof were introduced in frame with the LexA DNA binding domain in vector pBTM116 (Bartel and Fields, 1995). The coding sequences of *mep-1* derivatives were cloned into

pACTII in frame with the Gal4 activation domain (Bai and Elledge, 1997). All constructs were fully sequenced. Two-hybrid assays were performed in strain L40 (*ura-*) using 1 mg/ml of X-Gal (Bai and Elledge, 1997). Typically, filters were incubated for 2 hours at 30°C. Interactions reported on Fig. 4A were confirmed in the opposite configuration (i.e. with MOG-6 as a Gal4 ACT fusion), except for MEP-1(SH) and MEP-1(FL), because LEXA::MEP-1(SH) caused autoactivation of the reporter transgene, and LexA::MEP-1(FL) was not expressed in yeast (data not shown). The presence of fusion proteins was verified by western blotting.

For in-vitro protein-protein binding assays, full-length *mog-6* cDNA was cloned into pCITE (Novagen). [³⁵S]Met]-labeled MOG-6 protein was produced using TNT-coupled reticulocyte lysates (Promega). *mep-1* and *fbf-1* cDNAs were introduced into pGEX (Pharmacia) and Glutathione-S-Transferase (GST) fusion proteins were purified from BL21 *E. coli* after 90 minutes of induction with 0.5 mM IPTG. TX100 (0.1%) was added for the extraction of the FBF-1-GST fusion protein. Glutathione-Sepharose beads (Pharmacia) (50 µl) were added to the lysate and incubated for 30 minutes at room temperature. Beads were washed with 1× PBS. Equivalent amounts of beads and radiolabeled MOG-6 protein were incubated at 4°C under gentle rocking for 3 hours in binding buffer (20 mM HEPES pH 7.5, 75 mM KCl, 1 mM EDTA, 2 mM MgCl₂, 2 mM DTT, 0.5% NP-40). After several washes in binding buffer, retained proteins were eluted by boiling in sample buffer and were analyzed by SDS-PAGE and autoradiography. The input lane corresponds to 10% of the amount of radiolabeled protein used for each experimental lane.

RNA interference

mog-6/mIn1[dpy-10(e128)mIs14 GFP] hermaphrodites were grown at 25°C on HT115 bacteria producing both sense and antisense *gld-3* RNA strands (nt 327 to 766) (Timmons and Fire, 1998). DAPI-stained adults were scored for germline defects.

Nucleotide sequence accession number

The *mog-6* cDNA sequence data have been submitted to the DDBJ/EMBL/GenBank databases under accession number AF421146.

Results

mog-6 encodes a divergent cyclophilin

mog-6 was mapped on chromosome II, between *unc-4* and *sqt-1* (Fig. 1A). Deficiency mapping placed *mog-6* in a region that was covered by four cosmids (Fig. 1B). The phenotype of a *mog-6/mnDf90* heterozygote was identical to that of a *mog-6* homozygote, indicating that *mog-6(q465)* is a genetic null allele. *mog-6* was rescued by a pool of four cosmids (Fig. 1C, black bars), but also by cosmid M106 alone or by pAP6, a 3.1 kb fragment of M106 (Fig. 1D).

pAP6 was predicted to contain one single open reading frame (ORF) of 1575 nucleotides, 1239 of which were deleted in the *mog-6(q465)* allele. The deletion started 600 nucleotides downstream of the initiator codon and ended 61 nucleotides downstream of the stop codon (Fig. 1E). Along with the rescue analysis, the presence of this deletion strongly indicated that pAP6 corresponded to *mog-6*. A *mog-6* cDNA containing a coding region of 1575 nucleotides and UTRs of 1 and 50 nucleotides on the 5' and 3' end, respectively, was isolated. Although the cDNA was missing two nucleotides (A and T) in the 5' UTR, as well as the spliced leader, it nevertheless contained the entire ORF for the following reasons: (1) a splice acceptor site was located five nucleotides upstream of the translation initiation codon in the *mog-6* gene; (2) the initiation

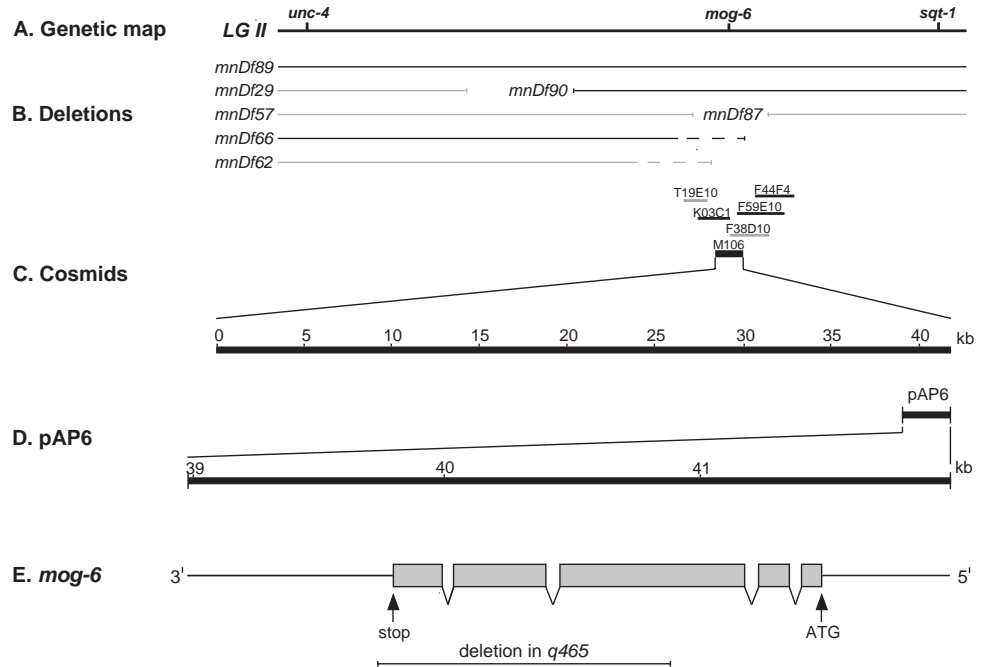


Fig. 1. Cloning of *mog-6*. (A) Genetic map. *mog-6* is located on chromosome II, between *unc-4* and *sqt-1*. (B) Deletion analysis. *mnDf66*, *mnDf89* and *mnDf90* (black) remove *mog-6* while *mnDf29*, *mnDf57*, *mnDf62* and *mnDf87* (gray) do not. The exact breakpoints of *mnDf62* and *mnDf66* have not been determined (dashed lines). (C) Cosmids tested for rescue (black bars); only M106 rescued *mog-6*. (D) Subcloning of M106. A 3.1 kb fragment (pAP6) of M106 rescued *mog-6* and contains one open reading frame. (E) The *mog-6* gene. 5' and 3' flanking regions are represented as lines, exons as gray boxes, introns as lines joining the exons.

codon was within a very good consensus sequence for translational start in *C. elegans*; and (3) the first methionine of MOG-6 and the following amino acids were conserved in closely related homologs (Page and Winter, 1998).

mog-6 codes for a protein that belongs to the family of cyclophilins (Fig. 2A). Cyclophilins are small proteins that bind Cyclosporin A (CsA) (Handschumacher et al., 1984) and catalyze protein folding (Lang et al., 1987). Cyclophilins are characterized by a conserved CBD that is required for both CsA-binding and protein-folding activities. In *mog-6(q465)*, the CBD and the C-terminus were deleted (Fig. 1E). To date, 17 cyclophilins have been identified in *C. elegans* (Ma et al.,

2002; Page et al., 1996; Zorio and Blumenthal, 1999). MOG-6 is a divergent cyclophilin in that it contains N-terminal and C-terminal extensions that are unique to MOG-6. Furthermore, MOG-6 contains only 12 out of 15 conserved residues that bind CsA (shown in bold in Fig. 2A) (Page et al., 1996). Thus, MOG-6 differs from the prevailing cyclophilins such as human CypA or *C. elegans* CYP-3 or CYP-7. MOG-6 has previously been described in the context of a wide characterization of *C. elegans* cyclophilins (Page et al., 1996). In this study, MOG-6 was named CYP-4 and had moderate protein-folding activity. hCYP-60, the human ortholog of MOG-6 is 46% identical and was isolated as a protein that binds to the proteinase inhibitor

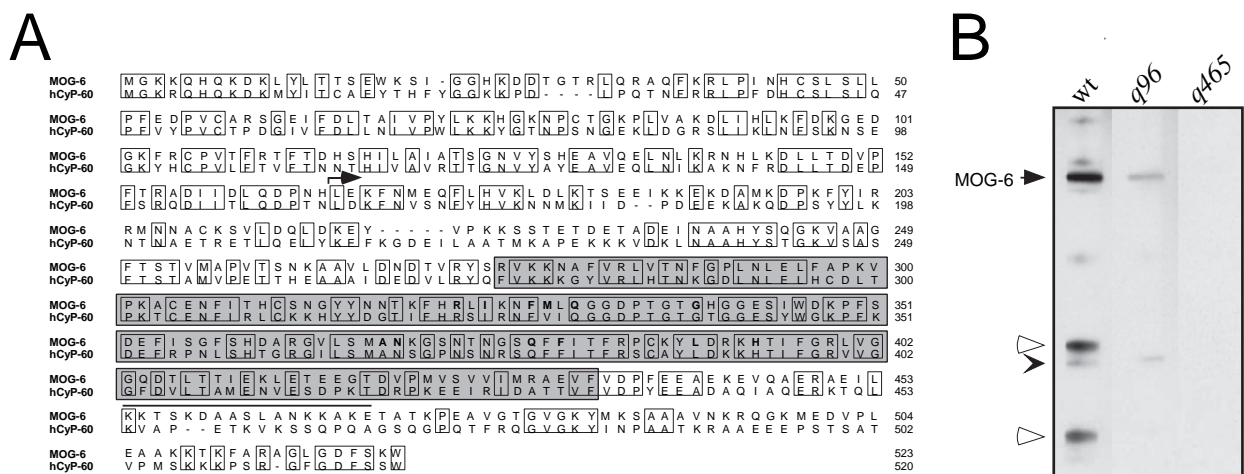
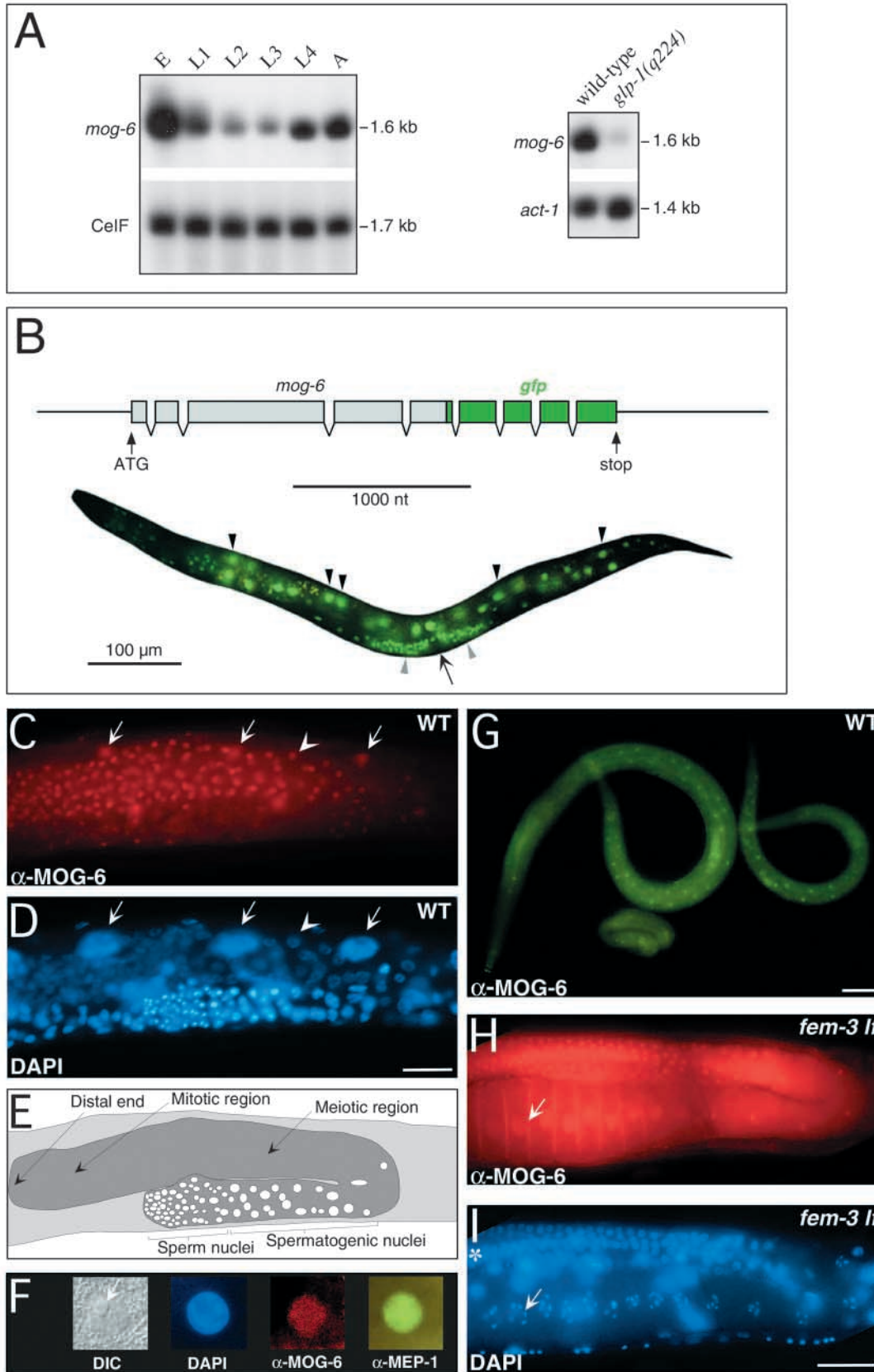


Fig. 2. (A) The MOG-6 protein. The CBD is highlighted in gray (AA275-434). Residues that are involved in Cyclosporin A (CsA)-binding in canonical cyclophilins are shown in bold. The nuclear localization signal is overlined. The starting point of the deletion in *mog-6(q465)* is shown by an arrow. The sequences of MOG-6 and of its human ortholog hCyp-60 are aligned. Conserved residues are boxed. (B) Western analysis. A 64 kD protein was detected with affinity-purified anti-MOG-6 antibodies in wild-type adults and masculinized adults (*fem-3(q96gf)*), but was absent in *mog-6(q465)* mutant adults. A minor 42 kD protein (open arrow) was absent in *q465* extracts but was also detected with preimmune serum (not shown). White arrowheads indicate cross-reacting bands that are oogenesis-dependent, since absent in masculinized animals.



peptide eglin c (Wang et al., 1996). In addition to the N- and C-terminal extensions, hCyP-60, MOG-6 and their close nematode orthologs share most residues of the CBD (Page and

Winter, 1998) (boxed in Fig. 2A). Furthermore, no closer homologs of hCyP-60 were found in the worm genome, indicating that MOG-6 is its *C. elegans* ortholog. Using anti-

Fig. 3. Expression of *mog-6*. (A) Northern analysis of *mog-6* RNA. (A, left) *mog-6* RNA levels vary throughout development: E, embryos; L1 to L4, larval stages; A, adult. CeIF was the loading control. Right, RNAs from adult wild-type and *glp-1* mutants were probed for *mog-6* and *act-1* (loading control). (B) Expression of *mog-6::gfp*. Top, the *mog-6* gene was fused in frame with *gfp*. Exons are represented by boxes. The 5' and 3' flanking sequences are those of *mog-6* (pAP6 in Fig. 1). Bottom, MOG-6::GFP is found in nuclei of the intestine (black arrowheads), uterus (gray arrowheads) and other somatic tissues. The black arrow points toward the vulva. Anterior is to the left. (C-I) Immunocytochemistry. (C) In wild-type L4 larvae, MOG-6 is expressed in germline nuclei throughout the mitotic and the meiotic regions. (D) To visualize nuclei, the same worm was stained with DAPI. Anti-MOG-6 antibodies stain somatic nuclei (intestine, white arrows in C,D) and mitotically or meiotically dividing germline nuclei (arrowhead in C,D). (E) Drawing of the germline shown in (C,D). Nuclei of sperm and spermatocytes are shown in white. (F) MOG-6 and MEP-1 in intestinal nuclei. The nucleolus is visible by DIC microscopy (arrow) and took up lower amounts of DAPI than the remainder of the nucleus. MOG-6 and MEP-1 are present throughout the whole nucleus, including the nucleolus. (G) MOG-6 in larvae. L3, left; L2 right; L1 before hatching, below. (H) Expression of MOG-6 in a feminized adult germline. MOG-6 is found in all nuclei, including those of mature oocytes (arrow). (I) DAPI staining of the same germline; the condensed chromosomes of accumulating oocytes are visible (white arrow). The asterisk shows the distal end of the germline. Scale bar: 20 μ m.

MOG-6 polyclonal antibodies, we detected a 64 kD protein in both wild-type and masculinized *fem-3(gf)* worms. The 64 kD protein most likely corresponded to native MOG-6, since it was of the expected size and was absent in *mog-6* mutants (Fig. 2B). The level of MOG-6 was reduced in the *fem-3(gf)* mutant, possibly because MOG-6 was also expressed in oocytes and embryos, which are absent in masculinized animals (see below).

***mog-6* is expressed in somatic and germline nuclei, but not in sperm**

To follow the expression of *mog-6* mRNA during development, poly(A)-enriched RNA from different developmental stages was isolated and analyzed by northern blotting. The *mog-6* transcript has a unique size of 1.6 kb (Fig. 3A). As predicted by its maternal-effect lethality (Graham et al., 1993), *mog-6* mRNA was abundant in embryos and its steady-state level decreased during larval development and rose during larval stage 4 and in the adult. Therefore the levels of *mog-6* mRNA varied during development in a manner that was predictable by its functions. In a temperature-sensitive *glp-1* mutant strain that hardly contained any germ cells, the level of the 1.6 kb transcript was dramatically reduced, while no significant changes were observed for actin-1 (Fig. 3A, right panel), indicating that the *mog-6* mRNA was present in the hermaphrodite germline, and to lesser extents in somatic tissues.

To follow the distribution of the MOG-6 protein in somatic tissues, we fused *mog-6* to the green fluorescent protein (*gfp*) gene (Fig. 3B). The *mog-6::gfp* reporter gene was expressed in many somatic cell nuclei, including those of the intestine, the pharynx and the uterus (Fig. 3B). A nuclear expression of MOG-6 was expected, because MOG-6 contains a nuclear localization signal (Fig. 2A).

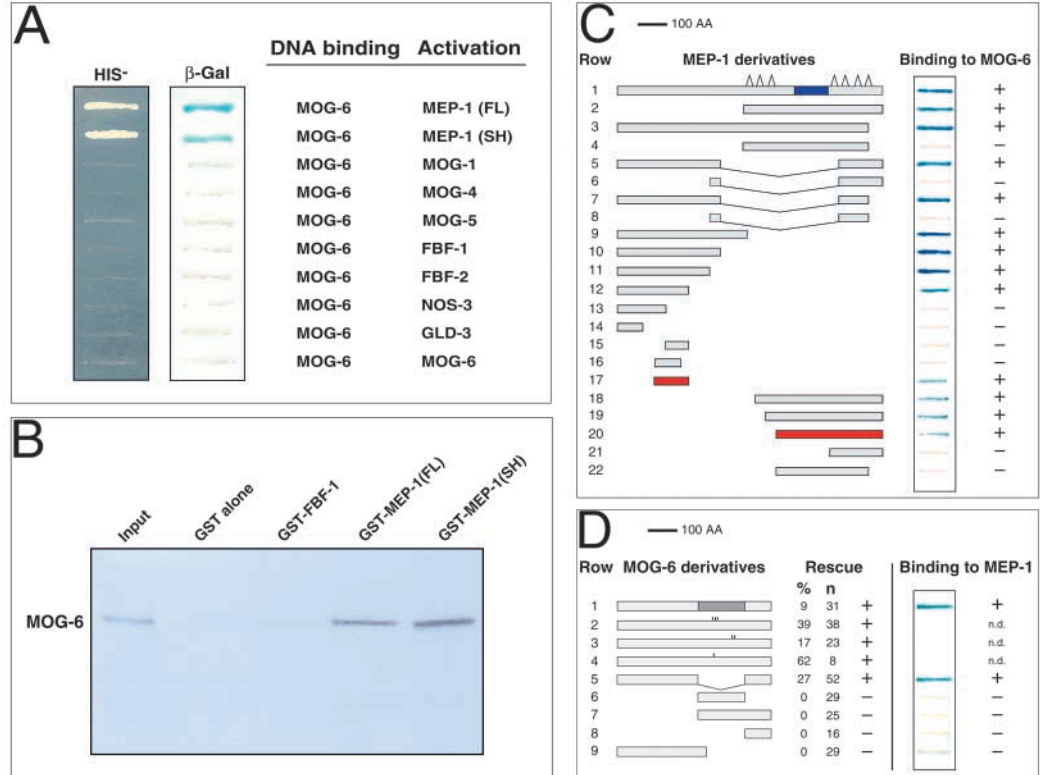
Transgenes that are expressed as multiple copies are silenced in the *C. elegans* germline (Seydoux and Schedl, 2001). Therefore in the germline, absence of MOG-6::GFP cannot be taken as indicative of *mog-6* expression. Moreover, northern analysis and the *Mog-6* mutant phenotype strongly indicated that MOG-6 was present in the germline. We therefore followed MOG-6 expression in the germline using anti-MOG-6 antibodies. Immunolocalization showed that MOG-6 was expressed in many nuclei of the germline and the soma (Fig. 3C,F). The germline of the *C. elegans* hermaphrodite is a syncytium made of two U-shaped arms (one arm is shown in dark gray in Fig. 3E). Mitotic divisions occur in the distal portion of the germline, while the proximal part contains mature gametes. We observed that in L4 larvae MOG-6 was ubiquitously expressed in the mitotic and meiotic regions but was absent in the proximal zone (Fig. 3C). Spermatozoa are formed from spermatocytes that divide twice to become haploid spermatids. Nuclei start to condense in secondary spermatocytes and are fully condensed in mature sperm (L'Hernaut, 1997). Co-staining with DAPI showed that MOG-6 was not expressed in primary and secondary spermatocytes, spermatids and mature sperm (Fig. 3C,D,E), but was present throughout the whole germline of a feminized adult (Fig. 3H,I). *fem-3* is required for spermatogenesis and is therefore expected to be expressed in sperm precursors. As a consequence, the distribution of MOG-6 correlates with its proposed role in *fem-3* repression. Consistent with the expression of MOG-6::GFP, we also found MOG-6 in intestinal nuclei (Fig. 3C, white arrows) and in somatic and germline nuclei of larvae at different developmental stages (Fig. 3G). Staining with anti-MOG-6 antibodies was absent in a *mog-6(q465)* mutant (not shown).

MOG-6 interacts with MEP-1

Previous studies have identified MEP-1 as a nuclear zinc finger protein that physically interacts with MOG-1, MOG-4 and MOG-5 (Belfiore et al., 2002). The nuclear coexpression of MOG-6 and MEP-1 (Fig. 3F) prompted us to check whether MOG-6 was able to physically interact with MEP-1. For this, we fused MOG-6 to the DNA-binding domain of LexA and tested its ability to interact with a Gal4(AD)MEP-1 fusion protein in the yeast two-hybrid system (Fields and Song, 1989). We found that MOG-6 interacted with full-length MEP-1 (MEP-1(FL)) and MEP-1(SH) (Fig. 4A, top rows). MEP-1(SH) lacks a large portion of its N-terminus but still retains the seven zinc fingers (Belfiore et al., 2002) (Fig. 4C, row 2). We found that MOG-6 did not bind to any of the other MOG proteins, nor to FBF, NOS-3 or GLD-3 (Fig. 4A, bottom rows). An independent yeast two-hybrid screen with MOG-6 as a bait confirmed the importance of the interaction between MOG-6 and MEP-1, since more than 70% of the cDNAs recovered were *mep-1* clones (data not shown). Yeast two-hybrid interactions were confirmed in a GST pulldown assay. MOG-6 was retained on full-length or short MEP-1, but neither on GST alone nor on FBF fused to GST (Fig. 4B). To exclude the possibility that an RNA derived from the in-vitro translation system could bridge MEP-1 and MOG-6 through unspecific protein-RNA interactions, we treated the in-vitro synthesized MOG-6 protein with RNase before incubation with GST-MEP-1. In all cases, the RNase did not reduce the amount of radiolabeled protein that was retained (data not shown).

Fig. 4. MOG-6 binds to MEP-1.

(A) Interaction assays between MOG-6 and additional regulators of *fem-3* in the yeast two-hybrid system. Growth on medium lacking histidine (left) or blue staining (right) represents positive interaction. MOG-6 was fused to the LexA DNA-binding domain, while the other proteins were fused to the Gal4 activation domain. Bottom lane, MOG-6 does not bind to itself. (B) Binding of MOG-6 to MEP-1 in vitro. MOG-6 bound to GST-MEP-1(FL) or GST-MEP-1(SH), but neither to GST alone nor to GST-FBF-1. (C) Functional domains in MEP-1. MEP-1(FL) is represented schematically in row 1: the Q-rich domain is shown as a blue box, and the zinc fingers are represented by vertical triangles. Row 2, MEP-1(SH) lacks the N-terminus (residues 1-407). Rows 3 to 22 represent other deletion derivatives of MEP-1. The shortest MEP-1 derivative that interacted with MOG-6



comprised 111 residues of the N-terminus (row 17, red box, residues 123 to 233) or 361 residues of the C-terminus (row 20, red box, AA 510 to 870). Internal deletions are shown by bars joining the N- and C-termini (rows 5 to 8). (D) *mog-6* rescue and MEP-1 binding. The complete *mog-6* gene and derivatives thereof were tested for *mog-6* rescue. The wild-type *mog-6* gene rescued *mog-6* (row 1, 9% rescue, $n=31$ rolling *unc-4mog-6* worms analyzed; self-fertile rolling Uncs were considered as rescued). *mog-6* constructions bearing point mutations in the CBD (bars in rows 2 to 4) or lacking the entire CBD (AA₂₇₅₋₄₃₄; row 5) rescued *mog-6* at least to the same extent as the wild-type *mog-6* gene. MOG-6 truncations retaining either the entire CBD (row 6), the CBD plus the C-terminus (row 7), or the C-terminus alone (row 8) did not rescue *mog-6*. Similarly, the entire N-terminal extension of MOG-6 did not rescue *mog-6* (row 9). MOG-6 derivatives were also assayed for MEP-1 binding in the yeast two-hybrid system. Right; MOG-6 requirements for MEP-1(FL) binding. Full length MOG-6 bound to MEP-1 (row 1, see also Fig. 4A). A MOG-6 protein that lacked the CBD interacted with MEP-1 (row 5), but neither the CBD alone (row 6), nor the CBD fused to the C-terminus (row 7) were sufficient for MEP-1 binding. If taken separately, the C- and N-termini of MOG-6 did not interact with MEP-1 (rows 8 and 9).

MEP-1 interacts with MOG-6 through two distinct domains

We used MEP-1 deletions to identify the domains through which MEP-1 interacts with MOG-6. MEP-1 is composed of an N-terminal extension and two sets of three and four zinc fingers, respectively, that surround a glutamine-rich domain (Q-domain) (Fig. 4C, row 1). The short MEP-1 isoform (row 2) was sufficient for MOG-6 binding but a deletion of the last 35 residues abolished this interaction (Fig. 4C, row 4). The same deletion had no effect on the interaction between MOG-6 and MEP-1(FL) (row 3), suggesting that MOG-6 and MEP-1(FL) bound through two independent domains, one located at the C-terminus and the other at the N-terminus. This idea was supported, in that N-terminal portions of MEP-1 did bind to MOG-6 (rows 9 to 12). However, MOG-6 binding was suppressed if fewer than 233 residues of the MEP-1 N-terminus were retained (233 residues in row 12; 155 in row 13). The shortest portion of the MEP-1 N-terminus that was sufficient for MOG-6 binding consisted of 111 amino acids (row 17). N- or C-terminal deletions of this fragment abolished the interaction with MOG-6 (rows 15 and 16).

To study the MOG-6 binding site in MEP-1(SH), we tested

the effect of C-terminal deletions. MEP-1(SH) interacted with MOG-6 (row 2) but did not if either the last 35 residues of its C-terminus (row 4) or the Q-domain and zinc fingers I to III were deleted (row 6). To ask whether the seven zinc fingers of MEP-1(SH) were all necessary for the interaction with MOG-6, we deleted the first cluster of zinc fingers of MEP-1(SH) (row 20). The corresponding protein bound to MOG-6, provided that the C-terminus was intact (compare rows 20 and 22). Deletion of the Q-domain and the first cluster of zinc fingers abolished MOG-6 binding (row 21). However, deletion of the first set of zinc fingers did not interfere with MOG-6 binding, as long as the Q-domain was intact (rows 18-20). In summary, we found that MOG-6 and MEP-1 interacted through two distinct domains in MEP-1, one that was located within residues 122 to 233 of MEP-1 (row 17, red box) and one that included the Q-domain, the second cluster of zinc fingers and the C-terminus (row 20, red box).

The CBD in MOG-6 is dispensable for sex determination and MEP-1 binding

Cyclophilins bind CsA and catalyze protein folding through the CBD (Kallen et al., 1991; Spitzfaden et al., 1992). We

wondered whether the CBD was necessary for MOG-6 function in worms. We therefore attempted to rescue *mog-6* with mutated forms of the *mog-6* gene. We tested three mutant MOG-6 proteins in which residues crucial for CsA binding and protein folding were changed to alanine. Substitution of R₃₂₃, F₃₂₈ and M₃₂₉ did not affect *mog-6* rescue (Fig. 4D, row 2). Similarly, L₃₉₀, H₃₉₄ and I₃₂₅ were not essential for MOG-6 function (rows 3 and 4). Importantly, a MOG-6 protein with a deleted CBD (AA₂₇₅₋₄₃₄) still rescued *mog-6* (row 5), while the CBD alone did not (row 6). Furthermore, if taken separately, the C-terminal (AA₄₃₅₋₅₂₃) and N-terminal domains of MOG-6 (AA₁₋₂₇₄) did not rescue *mog-6* on their own (rows 7 to 9). Our findings suggest that both the N- and C-termini of MOG-6, but not the CBD, are necessary and sufficient for MOG-6 function in vivo. The question that now arises is how does MOG-6 act on *fem-3* to regulate the sperm/oocyte switch? Since the CBD was dispensable for MOG-6 function, we propose that MOG-6 is unlikely to bind CsA or catalyze protein folding to achieve the sperm/oocyte switch. However, we have shown that MOG-6 bound to MEP-1 and, therefore, one possibility was that MEP-1 binding could be essential for MOG-6 function. We therefore tested different MOG-6 derivatives for MEP-1 binding. We found that the CBD was not required for MEP-1 binding, since a MOG-6 protein that was missing the CBD still bound efficiently to MEP-1 (row 5, right), whereas the CBD alone did not (row 6). If taken separately, the N- and C-termini of MOG-6 did not bind MEP-1 efficiently (rows 8 and 9). In summary, we found that both N- and C-terminal extensions of MOG-6 were necessary for MEP-1 binding and MOG-6 function.

No abnormal general splicing was detected in *mog-6* mutants

The findings that some cyclophilins are involved in pre-mRNA splicing (Bourquin et al., 1997; Horowitz et al., 1997; Teigelkamp et al., 1998) and that MOG-1, -4 and -5 are orthologs of well-characterized splicing factors (Puoti and Kimble, 1999; Puoti and Kimble, 2000) led us to consider the possibility that *mog-6* might control *fem-3* via regulated splicing. To this end, we analyzed several transcripts including *fem-3*, *fbf*, *nos-3* and *gld-3*. We analyzed each transcript by RT-PCR using primers that span the entire coding region. For *fem-3*, a 2.15 kb product was expected from unspliced RNA (Fig. 5A, lane 1). A 1.17 kb product that corresponded to fully spliced *fem-3* was obtained with poly(A)-enriched RNA from wild-type animals (Fig. 5A, lane 2), as well as from both wild-type (lane 6) and *mog-6* mutants (lane 4). The 1.17 kb product was absent if no reverse transcriptase was used, indicating that it corresponded to reverse-transcribed RNA (lanes 3 and 5). For *fbf-2*, the expected sizes of the unspliced and fully spliced RNAs were 2.1 and 1.83 kb, respectively (Fig. 5A, lanes 7 and 8). A 1.83 kb product was obtained from either *mog-6* or wild-type worms (lanes 10 and 12), indicating that *fbf-2* was correctly spliced in *mog-6* animals. A 2.59 kb product was obtained for the fully spliced *nos-3* mRNA, while the genomic fragment that contained four introns yielded a 3.07 kb PCR product. Again, no splicing defects were detected in *nos-3* (lanes 16 and 18). Since *fem-3*, *fbf-2* and *nos-3* are maternal mRNAs (Ahringer et al., 1992; Zhang et al., 1997; Kraemer et al., 1999), one possibility was that the RT-PCR products could have been generated from maternal RNAs that were provided

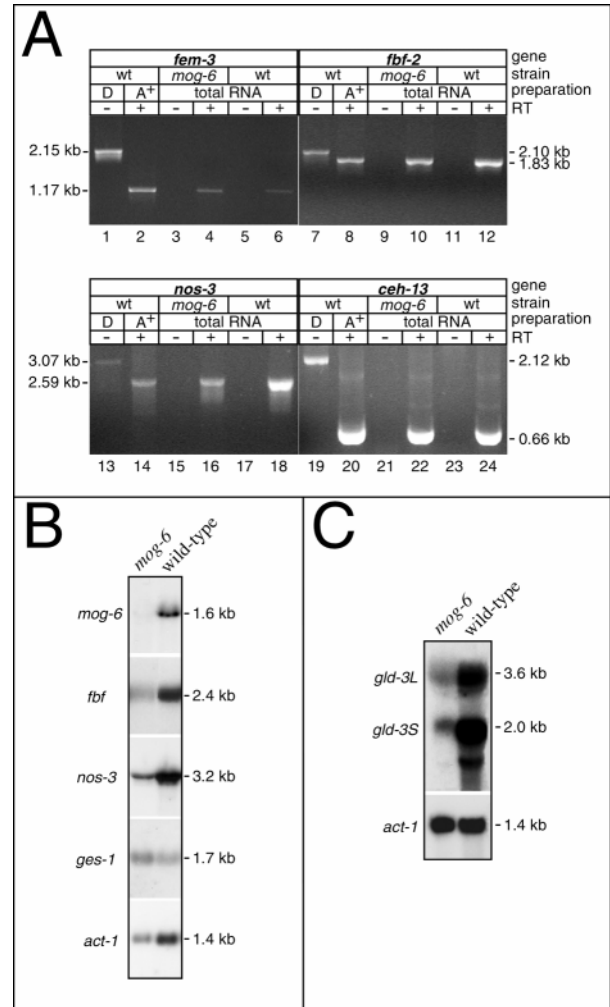


Fig. 5. Analysis of RNA splicing in *mog-6* mutants. (A) RT-PCR. Genomic DNA (D) or polyA-enriched RNA (A⁺) from wild-type worms were used as positive controls for PCR with sets of oligonucleotides specific for either *fem-3* (lanes 1 to 6), *fbf-2* (lanes 7 to 12), *nos-3* (lanes 13 to 18) or *ceh-13* (lanes 19 to 24). Total RNA from either *mog-6* or wild-type adults (wt) was used for PCR without (-) or with (+) RT. PCR on genomic DNA was used as a reference for the size of unspliced RNAs (lanes 1, 7, 13 and 19). (B) Northern analysis. Total RNA, 12.5 μ g, derived from adult *mog-6* or wild-type worms were run on a denaturing agarose gel and probed for *mog-6*, *fbf*, *nos-3*, *ges-1* and actin. (C) *gld-3* transcripts were analyzed on a separate blot loaded with 25 μ g and 50 μ g of total RNA from wild-type and *mog-6* mutants, respectively. The two major *gld-3* transcripts are indicated (Small and Large). Blots were also overexposed to ensure that no minor transcripts of abnormal size were present (not shown).

by the heterozygous mother. To rule out this possibility, we analyzed the *ceh-13* mRNA, which is zygotically expressed in early embryos and which is not contributed maternally (Wittmann et al., 1997). Splicing of *ceh-13* was normal in *mog-6* mutants, since only one 0.66 kb product that corresponded to fully spliced *ceh-13* mRNA was detected (Fig. 5, lanes 20 to 24). Splicing was also verified by northern blotting. The RNAs examined included *mog-6*, *fbf*, *nos-3*, *ges-1* and actin-1. *ges-1* is expressed in the soma from the 200-cell stage onward

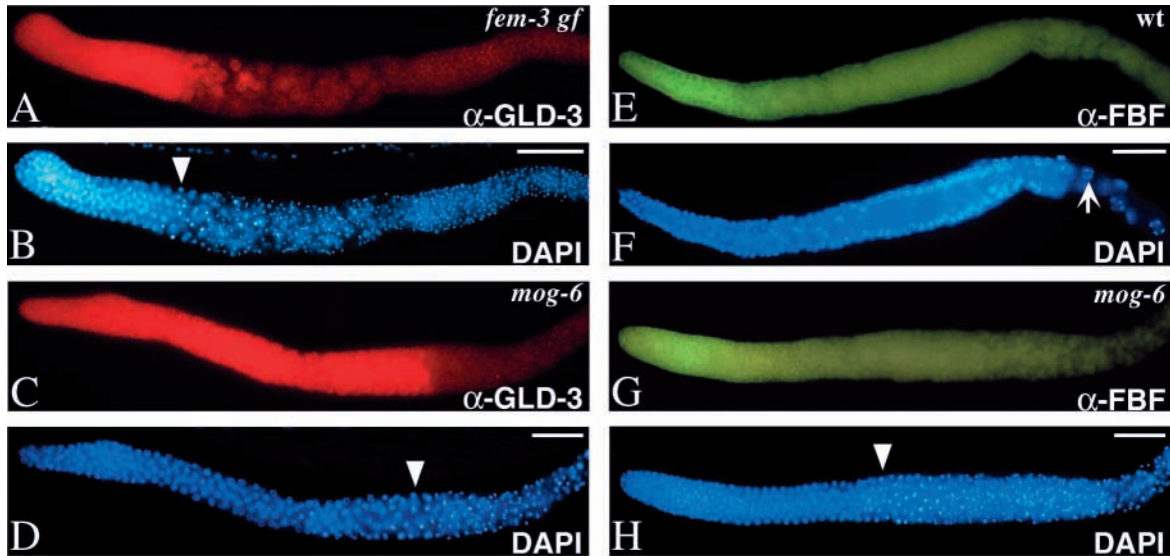


Fig. 6. *mog-6* is not required for the correct localization of GLD-3 and FBF. Germlines from adult hermaphrodites were immunostained for GLD-3 (A,C) and FBF (E,G). The corresponding DAPI stainings indicate the start of the spermatogenic region in masculinized mutants (shown to the right of white arrowheads in B,D,H). (E,F) Wild-type germlines produce oocytes in the proximal region (arrow). Scale bar: 20 μ m.

(Aamodt et al., 1991). The *mog-6* mRNA was absent in the *mog-6* mutant, and no transcript containing the corresponding deletion was detected, indicating that it is degraded (Fig. 5B, top). Germline-specific transcripts *fbf* and *nos-3* were of the same sizes in *mog-6* and wild-type animals, indicating that they were completely spliced (Fig. 5B). Since *fbf* and *nos-3* are abundant in embryos and oocytes, we expected a reduced signal in *mog-6* extracts (Kraemer et al., 1999; Zhang et al., 1997). *ges-1* and actin mRNAs also migrated to the expected size for fully spliced messengers (Fig. 5B, bottom). *gld-3* produces at least two major transcripts (Eckmann et al., 2002). Even if less abundant, probably because of the absence of embryos and oocytes, the large and small *gld-3* transcripts were detected in *mog-6* extracts and were of the expected sizes (Fig. 5C). In summary, among the transcripts analyzed, we did not detect abnormal products, indicating that general splicing occurred normally in *mog-6* animals.

***mog-6* is not required for the correct localization of other *fem-3* regulators**

FBF, GLD-3 and NOS-3 have been shown to function as cytoplasmic *trans*-acting regulators of the *fem-3* mRNA (Eckmann et al., 2002; Zhang et al., 1997; Kraemer et al., 1999). One possibility is that MOG-6 could repress *fem-3* by regulating the expression of such *trans*-acting factors. We therefore verified if GLD-3, FBF and NOS-3 were correctly expressed in *mog-6* animals. In wild-type animals, GLD-3 is expressed in the germline cytoplasm throughout the mitotic, transition and pachytene zones, in oocytes and primary spermatocytes (Eckmann et al., 2002). We stained masculinized *fem-3(gf)* germlines and found that GLD-3 was expressed throughout the mitotic and meiotic regions, but not in secondary spermatocytes (Fig. 6A,B). A similar expression pattern was observed in masculinized *mog-6* animals, with the one difference that the transition zone and pachytene region were larger than in *fem-3(gf)* animals (Fig. 6C,D), possibly

because the latter produced more sperm that filled the distal germline. FBF was present throughout the germline cytoplasm and was enriched in the mitotic region in hermaphrodites and males (Crittenden et al., 2002; Zhang et al., 1997) (Fig. 6E). We found that FBF expression was essentially similar in masculinized *mog-6* mutants and wild-type hermaphrodites, as it was detected in the mitotic and transition zones and decreased in germ cells that differentiate into oocytes or sperm (Fig. 6E,G). Like in masculinized *mog-6* hermaphrodites, FBF was not detected in the spermatogenic region in wild-type males, although it was present in the mitotic and meiotic regions (not shown). The localization of NOS-3 was similar to that of FBF, and we did not observe differences of NOS-3 expression in wild-type versus *mog-6* hermaphrodites (data not shown).

Taken together, our data suggest that *mog-6* does not regulate *fem-3* by modifying the expression of *trans*-acting regulators *gld-3*, *fbf* and *nos-3*.

Role of *mog-6* in the mitosis versus meiosis decision

Earlier studies have shown that *mog-1(0)* mutants produce fewer germ cells than normal (Puoti and Kimble, 1999). Similarly, *mog-6* animals also made reduced amounts of germ cells (1511 ± 117 , $n=22$ worms analyzed) compared with wild-type hermaphrodites that contain 2400 germ cells (Kimble and White, 1981). Even more significantly, *fog-1;mog-6* animals produced fewer oocytes (2.5 ± 0.7 , $n=45$ gonadal arms analyzed) than *fog-1* mutants (15.5 ± 2.8 , $n=21$), indicating that *mog-6* is required for robust germline proliferation.

In addition to their roles in germline sex determination, *nos*, *fbf* and *gld-3* are also required for germline survival (Subramaniam and Seydoux, 1999; Crittenden et al., 2002; Eckmann et al., 2002; Kraemer et al., 1999). We examined *mog-6 gld-3* double mutants to ask whether *mog-6* acted upstream of *gld-3* in germline sex determination, and whether

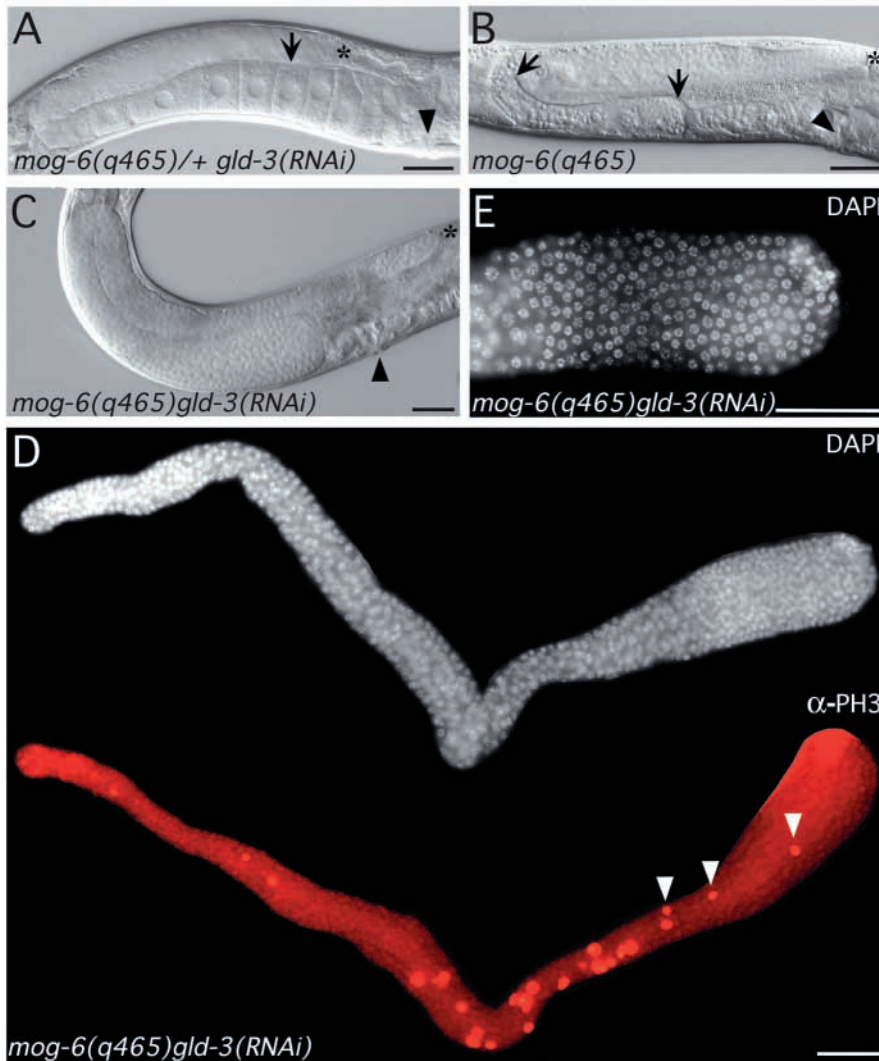


Fig. 7. *gld-3 mog-6* double mutants have tumorous germlines. Adult hermaphrodites were analyzed for germline phenotypes by DIC.

(A) *gld-3(RNAi)* caused feminization of *mog-6/+* heterozygotes (arrow points toward a stacking oocyte). (B) Germlines of *mog-6* homozygotes were masculinized (sperm is shown between the two arrows). (C) *gld-3(RNAi) mog-6* hermaphrodites are tumorous. (D) Dissected tumorous germline stained for DNA (top) or for the mitotic marker phosphohistone H3 (PH3) (bottom). Mitotic germ cells are present throughout the entire germline, including the proximal part of the germline (white arrowheads). The distal end is on the left. (E) Magnification of the proximal region shown in D (top) in a different focal plane. Asterisks indicate distal ends of germlines. Black arrowheads point toward the vulva. Scale bar: 20 μ m.

both genes interacted for germline proliferation. We found that *mog-6/mIn1;gld-3(RNAi)* heterozygotes made no sperm and accumulated oocytes (Fig. 7A). *mog-6* animals made only

Table 1. *mog;gld-3* double mutants

Hermaphrodites scored	Germline defects (%)						n
	Wild type (%)	sp only	oo only	sp+oo	tum	Other (Gls)	
<i>gld-3(RNAi)</i>	20	0	35	21	4	20	933
<i>mog-6(q465);gld-3(RNAi)</i>	0	32	1	1	54*	12	319
<i>mog-1(q223);gld-3(RNAi)</i>	0	47	1	1	44*	7	222
<i>mog-4(q233);gld-3(RNAi)</i>	0	40	1	6	40*	13	299
<i>mog-5(q449);gld-3(RNAi)</i>	0	52	3	1	35*	9	373
<i>mog-6(q465) gld-3(q730)</i>	0	0	0	0	100	0	173
<i>fem-3(q96gf);gld-3(RNAi)</i>	0	46	2	30	3	19	352

gld-3 mog double mutants form germline tumors. sp only, sperm only; oo only, oocyte-like germ cells only; sp+oo, sperm and oocyte-like germ cells; tum, tumorous germlines; other, other sterile phenotypes (including Gls, no germline in adults); n, number of adult worms scored.

* $P < 0.0001$. P values were obtained in a χ^2 -test by comparing the effect (i.e. tumorous and non tumorous germlines) of *gld-3(RNAi)* in wild-type versus *mog* mutant backgrounds.

sperm and had smaller germlines than *fem-3* gain-of-function mutants (Fig. 7B) (Barton et al., 1987; Graham et al., 1993). Surprisingly, germlines of *mog-6(q465) gld-3(RNAi)* animals were neither masculinized nor feminized, but tumorous (Tum), as they were filled with mitotically dividing germ cells (Fig. 7C-E; Table 1). Germline tumors were never observed in *mog-6* single mutants (0%, $n > 1000$). A very low incidence of Tum phenotypes was observed in *gld-3(q730)* or *gld-3(RNAi)* animals: 1% Tum ($n = 163$) and 4% Tum ($n = 933$), respectively. Germline tumors were also found in other *mog* mutants that were subjected to *gld-3(RNAi)* (Table 1). A completely penetrant Tum phenotype was observed in a genetic *mog-6(q465) gld-3(q730)* double mutant (Table 1). We asked whether the Tum phenotype was due to a masculinized germline, or rather to a defective *mog* gene. To this end, we analyzed the effect of *gld-3(RNAi)* in a masculinized *fem-3(gf)* germline, and found a majority of masculinized germlines, some partial feminization, but no significant amounts of Tum germlines (Table 1, last row). This finding suggests that *gld-3* and *mog* are synthetically required for meiosis.

Discussion

In this report, we show that *mog-6* codes for a divergent cyclophilin and that it plays an unexpected role in meiosis. After the identification of NinaA in *Drosophila*, MOG-6 is the second cyclophilin to be associated with a mutant phenotype in a developing organism (Shieh et al., 1989; Schneuwly et al., 1989; Baker et al., 1994).

MOG-6 is an unusual cyclophilin that binds to MEP-1

We found that MOG-6 interacted with MEP-1, which also binds to three other MOG proteins (Belfiore et al., 2002). Surprisingly, the MEP-1-MOG-6 interaction required both the N- and C-terminal domains of MOG-6, but not the conserved

CBD. Because the CBD was not necessary for MOG-6 in the sperm/oocyte switch as well, we propose that rather than the conserved CBD, the N- and C-terminal extensions of MOG-6 are essential for MOG-6 function and that this function might require the interaction between MOG-6 and MEP-1. Furthermore, MOG-6 has a reduced protein-folding activity (Page et al., 1996). We therefore propose that MOG-6 might not function as a normal cyclophilin in the sperm/oocyte switch.

What is the molecular role of MOG-6 in *fem-3* regulation? At present, we cannot answer this question in detail, but we nevertheless provide important insights. In this study, we show that MOG-6 is expressed in the nucleus of many somatic and germline cells, except in sperm and sperm precursors. The same expression pattern has been observed for MEP-1 (Belfiore et al., 2002), thus giving the opportunity for MEP-1 and MOG-6 to bind. An earlier study showed that in somatic tissues, *mog-6* was able to repress a transgene carrying the *fem-3* 3'UTR (Gallegos et al., 1998). The somatic expression of MOG-6 now explains the action of MOG-6 on the transgene.

Role of *mog-6* in germline proliferation

Maternal *mog-6* is needed for embryogenesis (Graham et al., 1993), thus suggesting a more general role of MOG-6 than solely germline sex determination. Like *gld-3*, *mog-6* is required for robust germline proliferation (Eckmann et al., 2002). However, *gld-3 mog-6* double mutants fail to produce sperm and develop tumorous germlines. The same phenotype was observed whenever the *gld-3* mutation was combined with *mog-1*, *-4* or *-5*, suggesting that *gld-3* and *mog* may function synthetically in the decision between mitosis and meiosis. At present, it is not clear whether mitotic proliferation occurs as a result of defective meiotic progression (Francis et al., 1995; Subramaniam and Seydoux, 2003), or as a result of a defective meiotic entry. Our data is consistent with the recent finding that both *nos-3 gld-2* and *nos-3 gld-3* double mutants also develop germline tumors (Hansen et al., 2004). The molecular role of the RNA-binding protein GLD-3 is not clear, but one possibility is that GLD-3 might bind to GLD-2 to control poly(A) tail extension of targets RNAs such as *gld-1* (Hansen et al., 2004; Wang et al., 2002). The implication of MOG in the mitosis/meiosis decision is not clear either. The MOG proteins could function synthetically with GLD-3 to control the expression of the *gld-1* RNA, but many other possibilities remain. Previous studies have shown that *fbf*, *nos*, *gld-2* and *gld-3* function not only in germline sex determination but also in the decision between meiosis and mitosis. We show now that at least *mog-1*, *-4*, *-5* and *-6* also play a dual role in germline fates.

Possible molecular roles of MOG-6

Many molecular functions have been attributed to cyclophilins, including RNA processing (Horowitz et al., 1997; Teigelkamp et al., 1998). We checked whether *mog-6* was required for the splicing of several mRNAs but did not detect unprocessed RNAs. A similar result was obtained in *mog-1* null mutants (Puoti and Kimble, 1999). If general pre-mRNA splicing was normal in *mog-6* mutants, what might be the role of *mog-6* in *fem-3* regulation? One possibility is that MOG-6 might indeed be required for splicing, but that its function would be

redundant with that of other proteins, perhaps another cyclophilin or MOG protein. Alternatively, *mog-6* might be necessary for splicing selected RNAs that are different from those tested. Many other possibilities remain. For instance, MOG-6 could be required for the localization of other factors such as FBF, NOS-3 and GLD-3 that in turn act on *fem-3* in the cytoplasm. However, we did not observe an altered expression pattern of FBF and GLD-3 in *mog-6* mutants. Another possibility is that MOG-6 is required for the biological activity of FBF, NOS-3 and GLD-3 rather than for their expression.

How does the MOG-6 protein control the sperm/oocyte switch? Its maternal requirement for embryonic development (Graham et al., 1993), its ubiquitous expression and its roles in both germline sex determination and proliferation indicate that *fem-3* is unlikely to be the unique target of *mog-6*. The identification of other proteins that genetically or physically interact with MOG-6, as well as the discovery of additional targets of *mog-6*, are likely to bring more insights.

We gratefully acknowledge Judith Kimble for providing the *mog-6* mutant and sharing antibodies against FBF, NOS-3 and GLD-3. We thank Tim Schedl for sharing unpublished results and for insightful comments. Thanks to Fabienne Hunston for comments on the manuscript. We acknowledge the CGC for strains, and the *C. elegans* Sequencing Consortium for providing fully sequenced cosmids. A.P. was supported by the Swiss National Science Foundation (grants 3100-67052.01 and 3130-054989.98).

References

- Aamodt, E. J., Chung, M. A. and McGhee, J. D. (1991). Spatial control of gut-specific gene expression during *Caenorhabditis elegans* development. *Science* **252**, 579-582.
- Ahringer, J. and Kimble, J. (1991). Control of the sperm-oocyte switch in *Caenorhabditis elegans* hermaphrodites by the *fem-3* 3'untranslated region. *Nature* **349**, 346-348.
- Ahringer, J., Rosenquist, T. A., Lawson, D. N. and Kimble, J. (1992). The *Caenorhabditis elegans* sex determining gene *fem-3* is regulated post-transcriptionally. *EMBO J.* **11**, 2303-2310.
- Bai, C. and Elledge, S. J. (1997). Searching for interacting proteins with the two-hybrid system I. In *The Yeast Two-Hybrid System* (ed. P. L. Bartel and S. Fields), pp. 11-28. Oxford, UK: Oxford University Press.
- Baker, E. K., Colley, N. J. and Zucker, C. S. (1994). The cyclophilin homolog NinaA functions as a chaperone, forming a stable complex in vivo with its protein target rhodopsin. *EMBO J.* **13**, 4886-4895.
- Bartel, P. L. and Fields, S. (1995). Analyzing protein-protein interactions using two-hybrid system. *Methods Enzymol.* **254**, 241-263.
- Barton, M. K., Schedl, T. B. and Kimble, J. (1987). Gain-of-function mutations of *fem-3*, a sex-determination gene in *Caenorhabditis elegans*. *Genetics* **115**, 107-119.
- Belfiore, M., Mathies, L. D., Pugnale, P., Moulder, G., Barstead, R., Kimble, J. and Puoti, A. (2002). The MEP-1 Zn-finger protein acts with MOG DEAH-box proteins to control gene expression via the *fem-3* 3'UTR in *C. elegans*. *RNA* **8**, 725-739.
- Bettinger, J. C., Lee, K. and Rougvie, A. E. (1996). Stage-specific accumulation of the terminal differentiation factor LIN-29 during *Caenorhabditis elegans* development. *Development* **122**, 2517-2527.
- Bourquin, J.-P., Stajlar, I., Meyer, P., Moosbaum, P., Silke, J., Baechi, T., Georgiev, O. and Schaffner, W. (1997). A Serine/arginine-rich nuclear matrix cyclophilin interacts with the C-terminal domain of RNA polymerase II. *Nucleic Acids Res.* **25**, 2055-2061.
- Crittenden, S. L., Bernstein, D. S., Bachorik, J. L., Thompson, B. E., Gallegos, M., Petcherski, A. G., Moulder, G., Barstead, R., Wickens, M. and Kimble, J. (2002). A conserved RNA-binding protein controls germline stem cells in *Caenorhabditis elegans*. *Nature* **417**, 660-663.
- Eckmann, C. R., Kraemer, B., Wickens, M. and Kimble, J. (2002). GLD-

- 3, a Bicaudal-C Homolog that Inhibits FBF to Control Germline Sex Determination in *C. elegans*. *Dev. Cell* **3**, 697-710.
- Fields, S. and Song, O.** (1989). A novel genetic system to detect protein-protein interactions. *Nature* **340**, 245-246.
- Fischer, G., Wittmann-Liebold, B., Lang, K., Kieffhaber, T. and Schmid, F. X.** (1989). Cyclophilin and peptidyl-prolyl *cis-trans* isomerase are probably identical proteins. *Nature* **237**, 476-478.
- Francis, R., Maine, E. and Schedl, T.** (1995). Analysis of the multiple roles of *gld-1* in germline development: interactions with the sex determination cascade and the *glp-1* signalling pathway. *Genetics* **139**, 607-630.
- Gallegos, M., Ahringer, J., Crittenden, S. and Kimble, J.** (1998). Repression by the 3' UTR of *fem-3*, a sex-determining gene, relies on a ubiquitous *mog*-dependent control in *Caenorhabditis elegans*. *EMBO J.* **17**, 6337-6347.
- Graham, P. L. and Kimble, J.** (1993). The *mog-1* gene is required for the switch from spermatogenesis to oogenesis in *Caenorhabditis elegans*. *Genetics* **133**, 919-931.
- Graham, P. L., Schedl, T. and Kimble, J.** (1993). More *mog* genes that influence the switch from spermatogenesis to oogenesis in the hermaphrodite germ line of *Caenorhabditis elegans*. *Dev. Genet.* **14**, 471-484.
- Handschumacher, R. E., Harding, M. W., Rice, J., Drugge, R. J. and Speicher, D. W.** (1984). Cyclophilin: a specific cytosolic binding protein for Cyclosporin A. *Science* **226**, 544-547.
- Hansen, D., Wilson-Berry, L., Dang, T. and Schedl, T.** (2004). Control of the proliferation versus meiotic development decision in the *C. elegans* germline through regulation of GLD-1 protein accumulation. *Development* **131**, 93-104.
- Horowitz, D. S., Kobayashi, R. and Krainer, A. R.** (1997). A new cyclophilin and the human homologues of yeast Prp3 and Prp4 form a complex associated with U4/U6 snRNPs. *RNA* **3**, 1374-1387.
- Jones, A. R., Francis, R. and Schedl, T.** (1996). GLD-1, a cytoplasmic protein essential for oocyte differentiation, shows stage- and sex-specific expression during *Caenorhabditis elegans* germline development. *Dev. Biol.* **180**, 165-183.
- Kallen, J., Spitzfaden, C., Zurini, M. G., Wider, G., Widmer, H., Wuthrich, K. and Walkinshaw, M.** (1991). Structure of human cyclophilin and its binding site for Cyclosporin A determined by X-ray crystallography and NMR spectroscopy. *Nature* **353**, 276-279.
- Kimble, J. E. and White, J. G.** (1981). On the control of germ cell development in *Caenorhabditis elegans*. *Dev. Biol.* **70**, 396-417.
- Kraemer, B., Crittenden, S., Gallegos, M., Moulder, G., Barstead, R., Kimble, J. and Wickens, M.** (1999). NANOS-3 and FBF proteins physically interact to control the sperm-oocyte switch in *Caenorhabditis elegans*. *Curr. Biol.* **9**, 1009-1018.
- L'Hernaut, S. W.** (1997). Spermatogenesis. In *C. elegans II* (ed. D. L. Riddle, T. Blumenthal, B. J. Meyer and J. R. Priess), pp. 271-294. Cold Spring Harbor, NY: Cold Spring Harbor Laboratory Press.
- Lang, K., Schmid, F. X. and Fischer, G.** (1987). Catalysis of protein folding by prolyl isomerase. *Nature* **329**, 268-270.
- Ma, D., Nelson, L. S., LeCoz, K., Poole, C. and Carlow, C. K. S.** (2002). A novel cyclophilin from parasitic and free-living nematodes with a unique substrate- and drug-binding domain. *J. Biol. Chem.* **277**, 14925-14932.
- Page, A. P. and Winter, A. D.** (1998). A divergent multi-domain cyclophilin is highly conserved between parasitic and free-living nematode species and is important in larval muscle development. *Mol. Biochem. Parasitol.* **95**, 215-227.
- Page, A. P., MacNiven, K. and Hengartner, M. O.** (1996). Cloning and biochemical characterization of the cyclophilin homologues from the free-living nematode *Caenorhabditis elegans*. *Biochem. J.* **317**, 179-185.
- Puoti, A. and Kimble, J.** (1999). The *Caenorhabditis elegans* sex determination gene *mog-1* encodes a member of the DEAH-box protein family. *Mol. Cell. Biol.* **19**, 2189-2197.
- Puoti, A. and Kimble, J.** (2000). The hermaphrodite sperm/oocyte switch requires the *Caenorhabditis elegans* homologs of PRP2 and PRP22. *Proc. Natl. Acad. Sci. USA* **97**, 3276-3281.
- Roussel, D. L. and Bennett, K. L.** (1992). *Caenorhabditis* cDNA encodes an eIF-4A protein. *Nucleic Acids Res.* **20**, 3783.
- Schedl, T.** (1997). Developmental genetics of the germ line. In *C. elegans II* (ed. D. L. Riddle, T. Blumenthal, B. J. Meyer and J. R. Priess), pp. 241-269. Cold Spring Harbor, NY: Cold Spring Harbor Laboratory Press.
- Schneuwly, S., Shortridge, R. D., Larrivee, D. C., Ono, T., Ozaki, M. and Pak, W. L.** (1989). *Drosophila ninaA* gene encodes an eye-specific cyclophilin (cyclosporin A binding protein). *Proc. Natl. Acad. Sci. USA* **86**, 5390-5394.
- Seydoux, G. and Schedl, T.** (2001). The germline in *C. elegans*: origins, proliferation and silencing. *Int. Rev. Cytol.* **203**, 139-185.
- Shieh, B.-H., Starnes, M. A., Seavello, S., Harris, G. L. and Zuker, C. S.** (1989). The *ninaA* gene required for visual transduction in *Drosophila* encodes a homologue of cyclosporin A-binding protein. *Nature* **338**, 67-70.
- Spitzfaden, C., Weber, H. P., Braun, W., Kallen, J., Wider, G., Widmer, H., Walkinshaw, M. D. and Wuthrich, K.** (1992). Cyclosporin A-cyclophilin complex formation. A model based on X-ray and NMR data. *FEBS Lett.* **300**, 291-300.
- Subramaniam, K. and Seydoux, G.** (1999). *nos-1* and *nos-2*, two genes related to *Drosophila nanos*, regulate primordial germ cell development and survival in *Caenorhabditis elegans*. *Development* **126**, 4861-4871.
- Subramaniam, K. and Seydoux, G.** (2003). Dedifferentiation of primary spermatocytes into germ cell tumors in *C. elegans* lacking the pumilio-like protein PUF-8. *Curr. Biol.* **13**, 134-139.
- Teigelkamp, S., Achsel, T., Mundt, C., Göthel, S.-F., Cronshagen, U., Lane, W. S., Mahariel, M. and Lührmann, R.** (1998). The 20kD protein of human [U4/U6.U5] tri-snRNPs is a novel cyclophilin that forms a ternary complex with the U4/U6-specific 60kD and 90kD proteins. *RNA* **4**, 127-141.
- Timmons, L. and Fire, A.** (1998). Specific interference by ingested dsRNA. *Nature* **395**, 854.
- Wang, B. B., Hayenga, K. J., Payan, D. G. and Fischer, J. M.** (1996). Identification of a nuclear-specific cyclophilin which interacts with the proteinase inhibitor eglin c. *Biochem. J.* **314**, 313-319.
- Wang, L., Eckmann, C., Kadyk, L., Wickens, M. and Kimble, J.** (2002). A regulatory cytoplasmic poly(A) polymerase in *Caenorhabditis elegans*. *Nature* **419**, 312-316.
- Wittmann, C., Bossinger, O., Goldstein, B., Fleischmann, M., Kohler, R., Brunschwig, K., Tobler, H. and Müller, F.** (1997). The expression of the *C. elegans labial-like Hox* gene *ceh-13* during early embryogenesis relies on cell fate and on anteroposterior cell polarity. *Development* **124**, 4193-4200.
- Zhang, B., Gallegos, M., Puoti, A., Durkin, E., Fields, S., Kimble, J. and Wickens, M. P.** (1997). A conserved RNA-binding protein that regulates sexual fates in the *C. elegans* hermaphrodite germ line. *Nature* **390**, 477-484.
- Zorio, D. A. R. and Blumenthal, T.** (1999). U2AF35 is encoded by an essential gene clustered in an operon with RRM/cyclophilin in *Caenorhabditis elegans*. *RNA* **5**, 487-494.